

AD-A048 328

CALIFORNIA INST OF TECH PASADENA
ELECTROOPTIC PHENOMENA AND DEVICES IN GASES.(U)
SEP 77 A YARIV

F/G 20/6

UNCLASSIFIED

ARO-13090.2-P

DAA629-75-6-0191
NL

AD-A048 328



AD A 048328

18 ARO 19 13090.2-P

6 ELECTROOPTIC PHENOMENA AND DEVICES.
IN GASES.

10
B.S.

9 Final Technical Report.

34 Jun 75 - 29 Jun 77

10 Amnon/Yariv, Principal Investigator

11 26 September 26, 1977

12 36p.

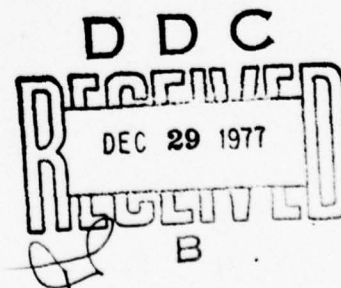
U. S. Army Research Office

15 Grant No. DAAG29-75-G-0191

California Institute of Technology, Pasadena, California

AD No. _____
DDC FILE COPY

Approved for public release;
distribution unlimited



1973
071 550

4B

TECHNICAL DISCUSSION

The grant period was devoted to a study of two classes of non-linear optical processes:

(1) Nonlinear optical mixing of microwave radiation at 4 GHz, with the 944 cm^{-1} P(20) line of CO_2 in a NH_2D gas. This analysis formed the basis for a series of experiments at the Hughes Research Laboratories, Malibu, where the effect was observed and agreement with the theory established.

The work is described in the enclosed reprint (Appendix 1).

(2) Conjugate four-wave mixing for time reversed propagation: A theoretical analysis of four-wave mixing in gases was conducted. Special emphasis is on the use of this effect for correcting for aberrations in optical propagation.

In addition, we carried out a theoretical study which treats all orders of nonlinear optical mixing phenomena, including Raman processes, using a unified point of view and introducing to nonlinear optics the formalism of Feynman diagrams. This study will be useful to identify candidate materials for resonantly enhanced four-wave mixing experiments described in (2) above. (See Appendix 2).

The research effort involved, in addition to the Principal Investigator, the full time of a graduate student, Pochi Yeh, who will obtain his PhD degree from Caltech for work supported by this grant.

White Section <input checked="" type="checkbox"/>	
Buff Section <input type="checkbox"/>	
UNANNOUNCED <input type="checkbox"/>	
JUSTIFICATION <input type="checkbox"/>	
BY _____	
DISTRIBUTION/AVAILABILITY CODES	
Dist.	AVAIL. and/or SPECIAL
A	

Stark-Induced Three-Wave Mixing in Molecular Gases—Part I: Theory

RICHARD L. ABRAMS, MEMBER IEEE, AMNON YARIV, FELLOW, IEEE, AND PO CHI A. YEH

Abstract—Application of a dc electric field to a gaseous system destroys the basic inversion symmetry and allows three-wave mixing processes to occur. A theoretical derivation of this effect under conditions of resonantly enhanced nonlinearities is given for a three-level system. Calculations are presented for mixing of a CO₂ laser with 4-GHz microwaves in the molecule NH₂D, producing single lower sideband radiation.

Manuscript received September 2, 1976. This work was supported in part by the Advanced Research Projects Agency, monitored by the Office of Naval Research, and in part by the Army Research Office, Durham, NC.

R. L. Abrams is with Hughes Research Laboratories, Malibu, CA 90265.

A. Yariv and P. Yeh are with the California Institute of Technology, Pasadena, CA 91109.

I. INTRODUCTION

NONLINEAR optical mixing in atomic vapors has been demonstrated for a number of different processes including third harmonic generation [1]–[4], dc-induced second-harmonic generation [5], [6], infrared upconversion [7], [8], and multiphoton generation of new wavelengths [9]. Resonant enhancement and phase matching of three-photon processes has led to rather impressive conversion efficiencies for certain interactions in atomic vapors [2]–[4]. In this paper we discuss three-wave mixing processes in molecules where resonant enhancement is achieved via Stark tuning of the molecular energy levels. This interaction and its subsequent experimental observation [10] suggest a new type of

electrooptical effect, namely single-sideband generation by applied microwave frequencies. A theoretical derivation and calculations of the interaction for a three-level system are presented here, specialized to the case of a particular molecule (NH_2D). The experimental observations are discussed in the following paper [10].

II. THEORY

The application of a dc electric field to a gas introduces a preferred spatial direction, thus destroying the inversion symmetry. The second-order-induced polarization amplitude can then be related to the product of the field (complex) amplitudes by

$$P_{\alpha}^{(2)} = \omega_1 - \omega_2 = d_{\alpha\beta\gamma}^{(2)} \omega_1 - \omega_2 E_{3\beta} E_{2\gamma}^* \quad (1)$$

Choosing the direction of the dc field as z , the allowed $d_{\alpha\beta\gamma}$ are d_{zzz} , d_{zii} , and d_{iiz} , where $i = x$ or y .

In searching for a candidate gas in which to observe the effect, one should look for: 1) molecules with a strong permanent dipole moment or 2) molecules which, in the presence of a dc field, acquire a large dipole moment so that the presence of the dc field constitutes an appreciable perturbation.

A molecule meeting criterion 2) is NH_2D . The molecule has, among others, the three levels shown in Fig. 1, which can be Stark-tuned into simultaneous resonance with the $P(20)$ line of the CO_2 laser [11]–[14] and microwave radiation near 4 GHz as shown. This should lead to a strong resonant mixing of the $P(20)$ line (of frequency $\omega_3/2\pi$) and the microwave field at $\omega_2/2\pi = 4$ GHz, giving rise to the difference frequency radiation at $\omega_1 = \omega_3 - \omega_2$ when the Stark field is near $E_{dc} = 3570$ V/cm. Levels 1 and 2 belong to the lowest vibrational state ($\nu_2 = 0$) and have molecular angular momentum quantum numbers $J = 4$ and $|M| = 4$. The subscripts 04 and 14 correspond to the standard asymmetric top designation [15]. The symbols a (asymmetric) and s (symmetric) refer to the parity of the inversion-split vibrational wave functions. The application of an electric field E_{dc} causes an admixture of the wave functions $|4_{04}a\rangle$ and $|4_{14}s\rangle$ which is due to a nonvanishing matrix element of the molecular dipole operator connecting the two states. This admixture, which will soon be shown to be responsible for the nonlinear mixing, disappears at zero dc field. The parameter Δ appearing in the expression for the wave functions corresponds to the energy splitting $E_2 - E_1$ between the two low-lying states and is given by

$$\Delta = [4|\langle 4_{04}a | \mu_z | 4_{14}s \rangle|^2 (E_{dc})^2 + \delta^2]^{1/2} \quad (2)$$

while the admixture wave functions are

$$|1\rangle = \frac{1}{\sqrt{2}} [\sqrt{1 + \delta/\Delta} |4_{04}a\rangle + \sqrt{1 - \delta/\Delta} |4_{14}s\rangle],$$

$$|2\rangle = \frac{1}{\sqrt{2}} [\sqrt{1 - \delta/\Delta} |4_{04}a\rangle - \sqrt{1 + \delta/\Delta} |4_{14}s\rangle]$$

where δ is the zero field splitting and μ_z is the projection of the molecular dipole operator along the direction of the dc field.

The expression for the nonlinear dipole moment of an NH_2D molecule depends on matrix elements which can be

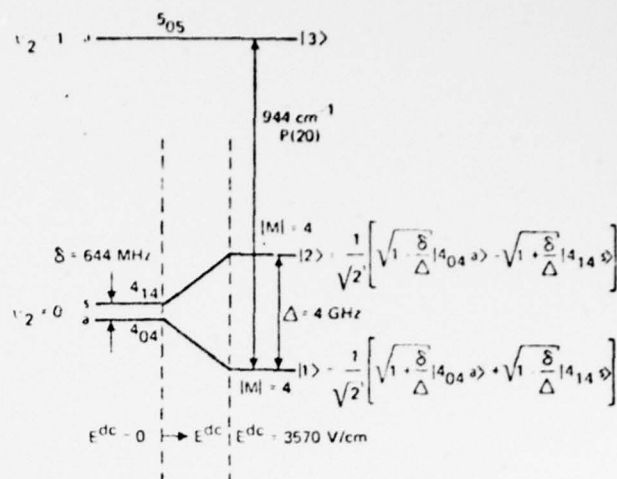


Fig. 1. Some of the energy levels relevant to the derivation of the nonlinear coefficient.

determined from linear absorption data as well as from the data on Stark splitting. This makes possible, in principle, a precise theoretical derivation of the nonlinear mixing behavior of this molecule and of its parametric dependencies.

Applying second-order perturbation theory [16, p. 556] to the three-level system of Fig. 1, and keeping only the resonant (i.e., with near vanishing denominator) term, leads to the following expression for the polarization generated at $\omega_1 = \omega_3 - \omega_2$ by the applied fields at ω_2, ω_3 :

$$P_{\alpha}^{(2)}(t) = \frac{1}{4\hbar^2} \left\{ \frac{N_1 (\bar{\mu} \cdot \bar{E}_3)_{13} (\bar{\mu} \cdot \bar{E}_2^*)_{21} (\mu_{\alpha})_{32}}{[\Gamma_{13} + i(\omega_3 - \omega_{31})] [\Gamma_{32} + i(\omega_1 - \omega_{32})]} - \frac{(N_2 - N_1) (\bar{\mu} \cdot \bar{E}_3)_{13} (\bar{\mu} \cdot \bar{E}_2^*)_{21} (\mu_{\alpha})_{32}}{[\Gamma_{12} + i(\omega_2 - \omega_{21})] [\Gamma_{32} + i(\omega_1 - \omega_{32})]} \right\} \exp(i\omega_1 t) + c.c. \quad (3)$$

where N_i is the population density of level i with $E_2 = E_3 = 0$. At thermal equilibrium $N_2 \approx N_1$, and the main contribution to $P_{\alpha}^{(2)}$ is from the first term, the one proportional to N_1 .

At zero dc field the matrix element $(\mu_{\alpha})_{32}$ is zero. This is due to the fact that, as can be shown by group theoretic arguments, only the molecular dipole moment along the b of NH_2D axis (μ_b) may possess a nonvanishing matrix element $\langle 5_{05}a | \mu_b | 4_{14}s \rangle$, but $\mu_b = 0$ due to the basal plane symmetry of NH_2D . It follows from (3) that for $E_{dc} = 0$ no frequency mixing takes place. When $E_{dc} \neq 0$ the ground state wave function $|4_{04}a\rangle$ is admixed into level 2 as shown in Fig. 1. This results in a nonvanishing matrix element $(\mu_{\alpha})_{32}$ proportional to $\langle 5_{05}a | \mu_{\alpha} | 4_{04}a \rangle$.

For $\bar{E}_2 \parallel \hat{z}$, $\alpha = x$, and $\bar{E}_3 \parallel \hat{x}$ we find, using the admixed wave functions, that the triple matrix element product appearing in (3) is given by

$$(\mu_z)_{21} (\mu_x)_{13} (\mu_x)_{32} = -4\mu_c \langle 4_{04}a | \mu_x | 5_{05}a \rangle^2 \cdot E_{dc} M^2 \left(\frac{\delta}{\Delta^2} \right) \quad (4)$$

The dependence of the triple matrix element product on the dc electric field is contained in the factor $E_{dc} \delta/\Delta^2$ with Δ the

energy separation between levels 2 and 1, as given by (2). The nonlinear mixing is thus absent, i.e., $P_x^{(2)} = 0$, at zero field ($E_{dc} = 0$) and at very high fields ($\Delta \gg \delta$). From (1) and (3) and using the fact that at room temperature $N_2 \approx N_1$, we obtain

$$d_{\alpha\beta\gamma}^{\omega_1=\omega_2-\omega_3} = \frac{1}{2\hbar^2} \frac{N_1(\mu_\gamma)_{21}(\mu_\beta)_{13}(\mu_\alpha)_{32}}{[\Gamma_{13} + i(\omega_3 - \omega_{31})][\Gamma_{32} + i(\omega_1 - \omega_{32})]} \quad (5)$$

Expression (5) applies to stationary molecules with energy levels at E_1 , E_2 , and E_3 . In a gas sample we need to account for the Doppler shift of the transition energies of individual molecules. This is done by averaging the nonlinear coefficient $d_{\alpha\beta\gamma}$ over the Maxwellian velocity distribution function with the result, for operation at line center, that

$$d_{\alpha\beta\gamma}^{\omega_1=\omega_2-\omega_3} = \frac{-N_1(\mu_\gamma)_{21}(\mu_\beta)_{13}(\mu_\alpha)_{32}}{2\hbar^2} \cdot \sqrt{\pi/2} \frac{c}{\sigma\omega_{31}} \frac{\partial F(x)}{\partial \Gamma} \quad (6)$$

where

$$F(x) = e^{x^2} \operatorname{erfc}(x), \quad \omega_{31} \approx \omega_{32} \gg \omega_{21}, \quad \Gamma_{13} \approx \Gamma_{32} \equiv \Gamma, \\ \sigma = \sqrt{kT/M}$$

is the rms molecular velocity, and $x = c\Gamma/(\sqrt{2}\sigma\omega_{31})$ is the ratio of the homogeneous (spontaneous plus pressure) linewidth Γ to the Doppler linewidth $\sqrt{2}\sigma\omega_{31}/c$.

Although a numerical estimate of the nonlinear mixing coefficient based on (6) is possible, a safer procedure, and one that serves as a check on the matrix elements needed to evaluate d_{xxz} (the largest coefficient in NH_2D) is to relate it to the linear absorption coefficient of x polarized field at $\omega_3 = \omega_{31}$. The latter can be shown to be given (in esu units) by

$$\gamma_{31} = \gamma_H \sqrt{\pi} x e^{x^2} \operatorname{erfc}(x) \quad (7)$$

where γ_H is the value of γ_{31} at high pressures ($c\Gamma \gg \sigma\omega_{31}$) and is given by

$$\gamma_H = \frac{4\pi|\mu_{13}|^2\omega_{31}}{\hbar c\Gamma} N_1.$$

Combining (6) and (7) leads after some mathematical manipulation to

$$d_{xxz}^{\omega_1=\omega_2-\omega_3} = -\frac{c(\mu_z)_{12}}{8\pi\hbar\omega_{31}} \left(\frac{\mu_{23}}{\mu_{13}} \right) \cdot \sqrt{\frac{\pi}{2}} \frac{c\gamma_H}{\sigma\omega_{31}} \left[2x^2 F(x) - \frac{2}{\sqrt{\pi}} x \right]. \quad (8)$$

The various constants in (8) are evaluated as follows: the matrix element $(\mu_z)_{12}$ is a function of the admixture and according to the wave functions (2) is given by

$$(\mu_z)_{12} = \frac{\delta}{\Delta} \langle a_{04} a | \mu_z | a_{14} s \rangle. \quad (9)$$

We obtain the matrix element $\langle a | \mu_z | s \rangle$ from comparing the splitting $E_2 - E_1$, as given by (2) to the experimental tuning

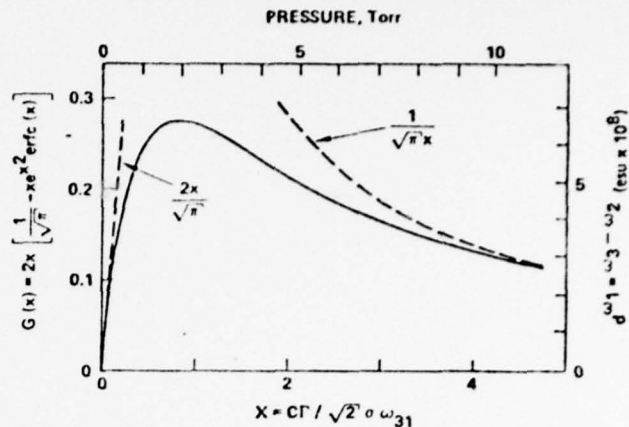


Fig. 2. Theoretical dependence of NH_2D nonlinear coefficient on pressure when the applied fields are exactly resonant with the Stark-tuned energy levels.

curve of $E_2 - E_1$ versus E_{dc} [14]. This yields $\langle a | \mu_z | s \rangle = 1.14 \times 10^{-18}$ esu. At resonance $E_{dc} = 3570$ V/cm and $\delta/\Delta = 0.174$. These data are used in (9) and result in

$$(\mu_z)_{12} = 0.174 \langle a | \mu | s \rangle = 0.198 \times 10^{-18} \text{ esu}.$$

The saturated absorption γ_H and pressure broadening coefficient are obtained from the data in [13] as

$$\gamma_H = 0.028 \text{ cm}^{-1}$$

$$\Gamma/P = 2\pi (20.1 \text{ MHz/torr}).$$

With these data we obtain

$$d_{xxz}^{\omega_1=\omega_2-\omega_3} = 2.31 \times 10^{-7} G(x) \text{ esu} \quad (10)$$

$$G(x) = 2x \left[\frac{1}{\sqrt{\pi}} - x e^{x^2} \operatorname{erfc}(x) \right]. \quad (11)$$

The theoretical dependence of d_{xxz} on pressure [see (10)] is plotted in Fig. 2. The peak occurs at $P = 2$ torr and has a value of

$$(d_{xxz}^{\omega_1=\omega_2-\omega_3})_{\max} = 6.4 \times 10^{-8} \text{ esu} = 2.4 \times 10^{-22} \text{ MKS}.$$

A comparison of this predicted behavior with experiment is given in [10].

The coefficient d estimated above refers to the generation of sideband radiation at ω_1 by mixing a CO_2 $P(20)$ line with a microwave field ω_2 (at 4.1 GHz). It is thus appropriate to compare it to the electrooptic coefficient r_{41} of GaAs which can be used, alternatively, to generate the sideband by conventional electrooptic modulation.

Using the correspondence [16, ch. 16]

$$r_{ijk} = -\frac{2\epsilon_0}{\epsilon_f \epsilon_l} d_{jkl} \quad (12)$$

we have

$$\frac{(n^3 r)_{\text{NH}_2\text{D}}}{(n^3 r)_{\text{GaAs}}} \sim 0.8. \quad (13)$$

We thus reach the conclusion that for sideband generation, dc-biased NH_2D at $P \approx 2$ torr is comparable to GaAs (which is

one of the best infrared modulation materials). We must recognize, however, that this large coefficient was obtained by exploiting the resonant nature of the effect. The penalty we pay for this is that of reduced bandwidth.

III. CONCLUSIONS

In conclusion, we have shown in detail how Stark admixing can give rise to second-order optical nonlinearities in gases. We have derived an expression for the coefficient describing the mixing of an infrared and a microwave field in NH_2D . Available absorption data were used to obtain a numerical estimate for the mixing and to describe its parametric dependence. An experimental demonstration of this effect is described in the following paper [10].

REFERENCES

- [1] J. F. Ward and G. H. C. New, "Optical third harmonic generation in gases by a focused laser beam," *Phys. Rev.*, vol. 185, pp. 57-72, Sept. 1969.
- [2] J. F. Young, G. C. Bjorklund, A. H. Kung, R. B. Miles, and S. E. Harris, "Third-harmonic generation in phase-matched Rb vapor," *Phys. Rev. Lett.*, vol. 27, pp. 1551-1553, Dec. 1971.
- [3] A. H. Kung, J. F. Young, G. C. Bjorklund, and S. E. Harris, "Generation of vacuum ultraviolet radiation in phase-matched Cd vapor," *Phys. Rev. Lett.*, vol. 29, pp. 985-988, Oct. 1972.
- [4] K. M. Leung, J. F. Ward, and B. J. Orr, "Two-photon resonant, optical third-harmonic generation in cesium vapor," *Phys. Rev.*, vol. 9A, pp. 2440-2448, June 1974.
- [5] R. S. Finn and J. F. Ward, "DC-induced optical second-harmonic generation in the inert gases," *Phys. Rev. Lett.*, vol. 26, pp. 285-289, Feb. 1971.
- [6] J. F. Ward and I. J. Bigio, "Molecular second- and third-order polarizabilities from measurements of second-harmonic generation in gases," *Phys. Rev.*, vol. 11A, pp. 60-66, Jan. 1975.
- [7] S. E. Harris and D. M. Bloom, "Resonantly two-photon pumped frequency converter," *Appl. Phys. Lett.*, vol. 24, pp. 229-230, Mar. 1974.
- [8] D. M. Bloom, J. Yardley, J. F. Young, and S. E. Harris, "Infrared up-conversion with resonantly two-photon pumped metal vapors," *Appl. Phys. Lett.*, vol. 24, pp. 427-428, May 1974.
- [9] P. D. Sorokin, J. J. Wynne, and J. R. Lankard, "Tunable coherent IR source based upon four-wave parametric conversion in alkali metal vapors," *Appl. Phys. Lett.*, vol. 22, pp. 342-344, Apr. 1973.
- [10] R. L. Abrams, C. K. Asawa, T. K. Plant, and A. E. Popa, "Stark-induced three-wave mixing in molecular gases—Part II: Experiment," this issue, pp. 82-85.
- [11] R. G. Brewer, M. J. Kelley, and A. Javan, "Precision infrared Stark spectra of $\text{N}^{14}\text{H}_2\text{D}$ using Lamb dip," *Phys. Rev. Lett.*, vol. 23, pp. 559-563, Sept. 1969.
- [12] M. J. Kelley, R. E. Francke, and M. S. Feld, "Rotational-vibrational spectroscopy of NH_2D using high-resolution laser techniques," *J. Chem. Phys.*, vol. 53, pp. 2979-2980, Oct. 1970.
- [13] T. K. Plant and R. L. Abrams, "Broadening and absorption coefficients in $\text{N}^{14}\text{H}_2\text{D}$," *J. Appl. Phys.*, vol. 47, pp. 4006-4008, Sept. 1976. Earlier data on this absorption coefficient and pressure broadening rate were published by A. R. Johnston and R. D. S. Melville, Jr., "Stark-effect modulation of a CO_2 laser by NH_2D ," *Appl. Phys. Lett.*, vol. 19, pp. 503-506, Dec. 1971, but the more recent measurements are more accurate and substantially different.
- [14] T. A. Nussmeier and R. L. Abrams, "Stark cell stabilization of CO_2 laser," *Appl. Phys. Lett.*, vol. 25, pp. 615-617, Nov. 1974.
- [15] C. H. Townes and A. L. Schawlow, *Microwave Spectroscopy*. New York: McGraw-Hill, 1955.
- [16] A. Yariv, *Quantum Electronics*, 2nd Ed. New York: Wiley, 1975.

APPENDIX 2

The Application of Time Evolution Operators and Feynman Diagrams to Nonlinear Optics *

Amnon Yariv

California Institute of Technology, Pasadena, California

ABSTRACT

The paper develops a consistent formalism for describing nonlinear optical mixing and multiphoton processes of any arbitrary order. The theory uses the time-evolution operators of quantum mechanics and the related, Feynman diagrams.

(To be published in the IEEE Journal of Quantum Electronics)

* Research supported by the U.S. Army Research Office.

I. General Background

The purpose of this note is to demonstrate the use of the quantum mechanical evolution operator formalism and the closely related technique of Feynman diagrams in deriving the nonlinear constants characterizing different multiphoton nonlinear optical processes.

As an illustration we apply the method to sum and frequency generation, two-photon absorption and stimulated Raman scattering. We start with a short review of the evolution operator formalism.⁽¹⁾

The eigenfunction $\psi(t)$ of an atom subjected to an electromagnetic field can be obtained formally by solving the Schrödinger equation

$$H\psi = i\hbar \frac{\partial \psi}{\partial t} \quad (1)$$

or, equivalently, by operating on the eigenfunction at time t_a with the evolution operator $u(t_b, t_a)$ according to

$$\psi(t_b) = u(t_b, t_a) \psi(t_a) \quad (2)$$

where $u(t_b, t_a)$ satisfies

$$i\hbar \frac{\partial u(t_b, t_a)}{\partial t_b} = H u(t_b, t_a) \quad (3)$$

If H does not depend on time, then it follows from (3) that

$$\begin{aligned} u(t_b, t_a) &= e^{-i \frac{H}{\hbar} (t_b - t_a)} \\ &= \sum_m |m\rangle \langle m| e^{-i\omega_m (t_b - t_a)} \end{aligned} \quad (4)$$

where $\omega_m \equiv E_m/\hbar$ and $|m\rangle$ is the eigenfunction of H with energy E_m , i.e., $H|m\rangle = \hbar\omega_m|m\rangle$.

In the cases of interest to us we take the Hamiltonian as

$$H(t) = H_0 + v(t) \quad (5)$$

where H_0 is time independent and $v(t)$ represents the time dependent interaction of the atom with the optical fields.

The solution of $u(t_b, t_a)$ when the Hamiltonian is given by (5) can be obtained by a perturbation expansion in powers of $v(t)$. The result is⁽¹⁾

$$u(t_b, t_a) = u^{(0)}(t_b, t_a) + u^{(1)}(t_b, t_a) + u^{(2)}(t_b, t_a) + \dots + u^{(n)}(t_b, t_a) + \dots \quad (6)$$

where

$$\begin{aligned} u^{(0)}(t_b, t_a) &= e^{-i \frac{H_0}{\hbar} (t_b - t_a)} \\ u^{(1)} &= \left(-\frac{i}{\hbar}\right) \int_{t_a}^{t_b} u^{(0)}(t_b, t) v(t) u^{(0)}(t, t_a) dt \\ u^{(2)} &= \left(-\frac{i}{\hbar}\right)^2 \int_{t_a}^{t_b} \int_{t_a}^{t_1} dt_1 dt_2 u^{(0)}(t_b, t_1) v(t_1) u^{(0)}(t_1, t_2) v(t_2) u^{(0)}(t_2, t_a) \end{aligned} \quad (7)$$

$$\begin{aligned} u^{(3)} &= \left(-\frac{i}{\hbar}\right)^3 \int_{t_a}^{t_b} \int_{t_a}^{t_1} \int_{t_a}^{t_2} dt_1 dt_2 dt_3 u^{(0)}(t_b, t_1) v(t_1) u^{(0)}(t_1, t_2) v(t_2) \\ &\quad \times u^{(0)}(t_2, t_3) v(t_3) u^{(0)}(t_3, t_a) \end{aligned}$$

where

$$t_b > t_1 > t_2 > t_3 \dots > t_n$$

The manner in which we are going to apply this formalism may be perhaps best illustrated by an example:

Consider the Raman scattering process in which an atom (or molecule), subjected to an optical field containing frequencies ω_1 and ω_2 and initially in the ground state n , absorbs a photon at ω_1 , while simultaneously emitting a photon at $\omega_2 < \omega_1$ while making a transition to state k . This process is illustrated in Fig. 1. Each scattering event results in the absorption of a photon at ω_1 and the emission of a photon at ω_2 . We may wish to calculate the rate at which ω_2 photons are generated per unit volume. This rate divided by the ω_2 photon flux (photons-m⁻²-sec⁻¹) gives us the exponential gain constant of the ω_2 field (the Raman gain).

We calculate the rate at which an atom makes the Raman transition $n \rightarrow k$ by taking the time derivative of the probability that an atom initially in the ground state n will be found at time t in state k . This probability is

$$\begin{aligned} P_k(t) &= |\langle k | \psi(t) \rangle|^2 \\ &= |\langle k | u(t,0) | n \rangle|^2 \end{aligned} \quad (8)$$

Since the basic scattering involves two photons, one at ω_1 and a second at ω_2 , we need to consider only the second order term, i.e., $u^{(2)}(t,0)$ so that

$$P_k(t) = |\langle k | u^{(2)}(t,0) | n \rangle|^2 \quad (9)$$

An alternative method would be to solve for the third order induced dipole moment of an atom subjected to fields $E_1 \exp(i\omega_1 t)$ and $E_2 \exp(i\omega_2 t)$. Specifically we are looking for an induced dipole moment which is proportional to

$$E_1 e^{i\omega_1 t} (E_1 e^{i\omega_1 t})^* E_2 e^{i\omega_2 t} = |E_1|^2 E_2 e^{i\omega_2 t} \quad (10)$$

Since the expectation dipole moment is given by

$$\langle \mu_i \rangle = \langle \psi(t) | \mu_i | \psi(t) \rangle \quad (11)$$

The desired dipole moment will result from terms such as $\langle \psi^{(1)} | \mu_i | \psi^{(2)} \rangle$, $\langle \psi^{(0)} | \mu_i | \psi^{(3)} \rangle$ where

$$\psi^{(n)}(t) \equiv u^{(n)}(t,0) \psi(0) \quad (12)$$

since they involve the third power of the perturbation, $v(t)$.

Using the first approach the power per unit volume generated at ω_2 is

$$P(\omega_2) = N W_{n \rightarrow k} \hbar \omega_2 \quad (13)$$

where

$$W_{n \rightarrow k} = \frac{d}{dt} P_k(t)$$

is the transition rate per atom from $|n\rangle$ to $|k\rangle$, and N is the density of atoms.

Using the second approach, i.e., the one leading to (11), we calculate the power $P(\omega_2)$ as

$$P(\omega_2) = \frac{1}{2} E_{2i} \overline{\frac{\partial}{\partial t} N \langle \mu_i \rangle} \quad (14)$$

where the bar denotes time averaging.

Either result, i.e., (13) or (14), can be obtained in a quick and straightforward manner using Feynman diagrams. This makes it possible to limit the considerations to resonant terms which dominate the process, when such terms exist, while ignoring the remaining terms.

By insisting that the results of (13) and (14) agree with each other we will learn how to include finite linewidths in the analysis.

To calculate the expectation value of physical observables as in (11) we need to obtain an expression for the wavefunction to any desired order of perturbation. The optical field at the atom site is taken as

$$\bar{E}(t) = \frac{1}{2} \bar{E}_1 e^{i\omega_1 t} + \frac{1}{2} \bar{E}_2 e^{i\omega_2 t} + \text{c.c.} \quad (15)$$

and the interaction Hamiltonian as

$$v(t) = -\bar{\mu} \cdot \left(\frac{\bar{E}_1}{2} e^{i\omega_1 t} + \frac{\bar{E}_2}{2} e^{i\omega_2 t} + \text{c.c.} \right) \quad (16)$$

The perturbation is assumed turned on at $t_0 = -\infty$ at which time the atom is in its ground state n . The eigenfunction at a subsequent time t is

$$\psi(t) = \psi^{(0)}(t) + \psi^{(1)}(t) + \dots \psi^{(n)}(t) + \dots \quad (17)$$

where from (2) and (6)

$$\psi^{(n)}(t) = u^{(n)}(t, t_0) |n\rangle \quad (18)$$

Using (7) we write

$$\begin{aligned} \psi^{(0)}(t) &= e^{-\frac{H_0}{\hbar}(t-t_0)} |n\rangle = e^{-i\omega_n(t-t_0)} |n\rangle \\ \psi^{(1)}(t) &= -\frac{i}{\hbar} \int_{t_0}^t e^{-\frac{iH_0}{\hbar}(t-t_1)} v(t_1) e^{-\frac{iH_0}{\hbar}(t_1-t_0)} dt_1 |n\rangle \end{aligned} \quad (19)$$

which using (4) becomes

$$\psi^{(1)}(t) = -\frac{i}{\hbar} \sum_m \int_{t_0}^t |m\rangle \langle m| e^{-i\omega_m(t-t_1)} v(t_1) e^{-i\omega_n(t_1-t_0)} |n\rangle dt_1 \quad (20)$$

Since $v(t_1)$ is, according to (16), a sum of four terms, the integrand in

(20) is made up of four terms. One such term, for example, resulting from the part of $v(t)$ involving $E_1^* \exp(-i\omega_1 t)$ will yield

$$\begin{aligned}\psi^{(1)}(t) &= \frac{i}{2\hbar} \sum_m \int_{t_0 \rightarrow -\infty}^t (\mu_1)_{mn} E_1^* e^{i(\omega_{mn}-\omega_1)t_1} e^{-i\omega_{mn}t} e^{i\omega_{mn}t_0} dt_1 |m\rangle \\ &= \frac{1}{2\hbar} \sum_m (\mu_1)_{mn} E_1^* \frac{e^{i(-\omega_1-\omega_n)t}}{\omega_{mn}-\omega_1-i\gamma} |m\rangle\end{aligned}\quad (21)$$

where μ_1 is the projection of $\bar{\mu}$ along \bar{E}_1 . In (21) we added the usual convergence factor γ by letting $\omega_m \rightarrow \omega_m - i\gamma$. The factor γ is then allowed to approach zero. This causes the integral at $t=-\infty$ to be zero. We will show later that if we leave γ as in (21) it will account correctly for the finite lifetime or linewidths of the transition. The constant factor $\exp(i\omega_{mn}t_0)$ has been left out since it cancels out (through multiplication by its complex conjugate) in the calculation of physical observables. As mentioned above $\psi^{(1)}(t)$ has three more terms each of a form similar to (21) but involving $+\omega_1$, $-\omega_2$ and $+\omega_2$. These arise from using the remaining three terms of the Hamiltonian (16) in (20). We thus have

$$\begin{aligned}\psi^{(1)}(t) &= \frac{1}{2\hbar} \sum_m \left\{ (\mu_1)_{mn} \frac{E_1^* e^{i(-\omega_1-\omega_n)t}}{\omega_{mn}-\omega_1-i\gamma} |m\rangle + (\mu_1)_{mn} \frac{E_1 e^{i(\omega_1-\omega_n)t}}{\omega_{mn}+\omega_1-i\gamma} |m\rangle \right. \\ &\quad \left. + (\mu_2)_{mn} \frac{E_2^* e^{i(-\omega_2-\omega_n)t}}{\omega_{mn}-\omega_2-i\gamma} |m\rangle + (\mu_2)_{mn} \frac{E_2 e^{i(\omega_2-\omega_n)t}}{\omega_{mn}+\omega_2-i\gamma} |m\rangle \right\}\end{aligned}\quad (22)$$

Using (7) we write the second order wavefunction $\psi^{(2)}(t)$ as

$$\begin{aligned}
\psi^{(2)}(t) &= u^{(2)}(t, t_0) |n\rangle = \\
& \left(-\frac{i}{\hbar}\right)^2 \int_{t_0}^t \int_{t_0}^{t_1} dt_1 dt_2 e^{-iH_0(t-t_1)} v(t_1) e^{-iH_0(t_1-t_2)} v(t_2) e^{-iH_0(t_2-t_0)} |n\rangle \\
&= \left(-\frac{i}{\hbar}\right)^2 \sum_m \sum_s \int_{t_0}^t \int_{t_0}^{t_1 > t_2} e^{-i\omega_s(t-t_1)} |s\rangle \langle s| v(t_1) e^{-i\omega_m(t_1-t_2)} |m\rangle \\
&\quad \times \langle m| v(t_2) e^{-i\omega_n(t_2-t_0)} |n\rangle dt_2 dt_1 \quad (23)
\end{aligned}$$

Since $v(t)$ contains four frequency terms and appears twice in (23) the full integration in (23) will yield 16 terms. A typical term, as an example involving the use of $-\mu_1 E_1^* e^{-i\omega_1 t_2}$ at t_2 and $-\mu_2 E_2^* e^{-i\omega_2 t_1}$ at t_1 is

$$\psi_{-\omega_1, -\omega_2}^{(2)}(t) = \sum_m \sum_s \left(\frac{1}{\hbar}\right)^2 \frac{E_1^* E_2^*}{4} \frac{(\mu_1)_{mn} (\mu_2)_{sm} e^{i(-\omega_n - \omega_1 - \omega_2)t}}{(\omega_{mn} - \omega_1 - i\gamma)(\omega_{sn} - \omega_1 - \omega_2 - i\gamma)} |s\rangle \quad (24)$$

A convenient way to represent (24) is through the use of a Feynman diagram as shown in Fig. 2. Time increases from the bottom to the top. Each solid line segment represents an eigenstate. The atom starts at t_0 in state n , scatters at t_2 into state m by absorbing a photon at ω_1 . This scattering is accounted for by the factor $(\mu_1)_{mn} E_1 e^{-i\omega_1 t} / (\omega_{mn} - \omega_1 - i\gamma)$ in (24). The next "scattering" is at t_1 and involves an absorption of a photon at ω_2 . A negative frequency denotes absorption and is represented by an arrow terminating at a corner, while an arrow starting at a corner denotes the emission of a photon. A case where the transition from state n to s involves the absorption of a photon at ω_1 and the emission of a photon at ω_2 , as an example, is shown in Fig. 2b.

The corresponding contribution to $\psi^{(2)}(t)$ can be written by inspection

$$\psi_{-\omega_1, \omega_2}^{(2)} = \sum_m \sum_s \left(\frac{1}{\hbar}\right)^2 \frac{E_1^* E_2}{4} \frac{(\mu_1)_{mn} (\mu_2)_{sm} e^{i(-\omega_n - \omega_1 + \omega_2)t}}{(\omega_{mn} - \omega_1 - i\gamma)(\omega_{sn} - \omega_1 + \omega_2 - i\gamma)} |s\rangle \quad (25)$$

We note that each scattering, i.e., each corner in the diagram contributes one factor to the denominator and the factor is equal to the energy in units of \hbar of the atom and field after the scattering minus the initial ($t = t_0$) energy. The second factor in the denominator in (25), as an example, is obtained from $\omega_s + \omega_2 - (\omega_1 + \omega_n)$. The remaining fourteen wavefunctions are obtained by taking all the possible permutations of $\psi_{\pm\omega_i, \pm\omega_j}^{(2)}$, $i, j = 1, 2$ where our convention is such that $\psi_{+\omega_i, -\omega_j}^{(2)}$, for example, corresponds to emitting an ω_i photon at t_2 and absorbing an ω_j photon at t_1 ($t_1 > t_2$). We note that $\psi_{-\omega_j, \omega_i}^{(2)}$ is not equal to $\psi_{\omega_i, -\omega_j}^{(2)}$.

Using the diagram technique we can write the wavefunction to any order of perturbation. As an example consider the process in which an atom makes a transition from state n to state s while absorbing one photon at ω_1 , one photon at ω_2 and emitting a photon at ω_3 . One diagram describing this process is $\psi_{-\omega_1, -\omega_2, \omega_3}^{(3)}$ as shown in Fig. 2c. We obtain by inspection

$$\psi_{-\omega_1, -\omega_2, \omega_3}^{(3)} = \sum_m \sum_k \sum_s \frac{-E_1^* E_2^* E_3}{8\hbar^3} \frac{(\mu_1)_{mn} (\mu_2)_{km} (\mu_3)_{sk} e^{i(-\omega_n - \omega_1 - \omega_2 + \omega_3)t}}{(\omega_{mn} - \omega_1)(\omega_{kn} - \omega_1 - \omega_2)(\omega_{sn} - \omega_1 - \omega_2 + \omega_3)} |s\rangle \quad (26)$$

The total number of $\psi_{\pm\omega_i, \pm\omega_j, \pm\omega_k}^{(3)}$ combinations is $6^3 = 216$. The tremendous advantage of the diagrammatic representation is that it enables us to single out and then treat very simply the terms which dominate in any given physical situation. This will become clearer in the examples which follow.

11. Frequency Addition

In this section we will calculate the nonlinear susceptibility $d_{ijk}^{\omega_3=\omega_1+\omega_2}$ which describes via the relation

$$P_i^{\omega_3=\omega_1+\omega_2} = d_{ijk}^{\omega_3=\omega_1+\omega_2} E_2 E_1 \quad (27)$$

The induced polarization along the i direction

$$P_i(t) = \text{Re} \left(P_i^{\omega_3=\omega_1+\omega_2} e^{i\omega_3 t} \right) \quad (28)$$

due to input fields $\text{Re} \left(E_{1j} e^{i\omega_1 t} \right)$ and $\text{Re} \left(E_{2k} e^{i\omega_2 t} \right)$ polarized along j and k , respectively.

The total atomic dipole moment is obtained from

$$\langle \mu_i(t) \rangle = \langle \psi(t) | \mu_i | \psi(t) \rangle \quad (29)$$

so that contributions containing the electric field to second power as in (27) must come from

$$\langle \mu_i^{(2)}(t) \rangle = \langle \psi^{(0)} | \mu_i | \psi^{(2)} \rangle + \langle \psi^{(2)} | \mu_i | \psi^{(0)} \rangle + \langle \psi^{(1)} | \mu_i | \psi^{(1)} \rangle \quad (30)$$

Each term in (30) contributes two terms to the desired polarization--one in which E_1 scatters first and then E_2 , and vice versa.

Consider as an example the terms due to $\langle \psi^{(1)} | \mu_i | \psi^{(1)} \rangle$:

$$\begin{aligned} \langle \psi^{(1)} | \mu_i | \psi^{(1)} \rangle &= \\ \sum_s \sum_m \frac{1}{4\hbar^2} \langle s | E_2(\mu_k)_{sn} \frac{e^{i(\omega_2+\omega_n)t}}{\omega_{sn}-\omega_2+i\gamma} | \mu_i | E_1(\mu_j)_{mn} \frac{e^{i(\omega_1-\omega_n)t}}{\omega_{mn}+\omega_1-i\gamma} | m \rangle & \\ = \sum_s \sum_m \frac{E_1 E_2}{4\hbar^2} \frac{(\mu_k)_{sn} (\mu_i)_{sm} (\mu_j)_{mn}}{(\omega_{sn}-\omega_2+i\gamma)(\omega_{mn}+\omega_1-i\gamma)} e^{i(\omega_1+\omega_2)t} & \end{aligned}$$

Note that any constant premultiplying a wavefunction to the left of μ_i is replaced by its complex conjugate. Collecting all the terms contributing to d_{ijk} yields

$$d_{ijk}^{\omega_3=\omega_1+\omega_2} = \frac{N}{2\hbar^2} \sum_m \sum_s \left[\frac{(\mu_k)_{sn}(\mu_i)_{sm}(\mu_j)_{mn}}{(\omega_{sn}-\omega_2+i\gamma)(\omega_{mn}+\omega_1-i\gamma)} + \frac{(\mu_j)_{sn}(\mu_i)_{sm}(\mu_k)_{mn}}{(\omega_{sn}-\omega_1+i\gamma)(\omega_{mn}+\omega_2-i\gamma)} \right. \\ + \frac{(\mu_j)_{mn}(\mu_k)_{sm}(\mu_i)_{ns}}{(\omega_{mn}+\omega_1-i\gamma)(\omega_{sn}+\omega_1+\omega_2-i\gamma)} + \frac{(\mu_k)_{mn}(\mu_j)_{sm}(\mu_i)_{ns}}{(\omega_{mn}+\omega_2-i\gamma)(\omega_{sn}+\omega_1+\omega_2-i\gamma)} \\ \left. + \frac{(\mu_j)_{nm}(\mu_k)_{sm}(\mu_i)_{ns}}{(\omega_{mn}-\omega_1+i\gamma)(\omega_{sn}-\omega_1-\omega_2+i\gamma)} + \frac{(\mu_k)_{nm}(\mu_j)_{sm}(\mu_i)_{ns}}{(\omega_{mn}-\omega_2+i\gamma)(\omega_{sn}-\omega_1-\omega_2+i\gamma)} \right]$$

A more conventional derivation is given in References (2), (3) and (4).

III. Two-Photon Absorption

Here we will apply our formalism to derive the transition rate for absorption of two photons--one at ω_1 and a second at ω_2 --by an atom. By allowing $\omega_1 = \omega_2$ we will get the familiar expression for two-photon absorption coefficient.

We start by writing the second order wavefunction $\psi^{(2)}(t)$ corresponding to an atom which at $t=0$ is at state n and which interacts with the radiation field, Eq. (15), consisting of fields at ω_1 and ω_2 . We will assume that the largest contribution to $\psi^{(2)}$ comes from $\psi_{-\omega_1, -\omega_2}^{(2)}$ corresponding to the diagram of Fig. 3. We write by inspection

$$\psi_{-\omega_1, -\omega_2}^{(2)}(t) = \sum_m \sum_s \left(\frac{E_1^* E_2^*}{4\hbar^2} \right) \frac{(\mu_1)_{mn}(\mu_2)_{sm}}{(\omega_{mn}-\omega_1)(\omega_{sn}-\omega_1-\omega_2)} e^{-i\omega_s t} \left[e^{i(\omega_{sn}-\omega_1-\omega_2)t} - 1 \right] |s\rangle \quad (31)$$

The -1 term is due to the fact that here we integrated from 0 to t . Let us assume that for some level m , $\omega_{mn} \approx \omega_1$ so the term m dominates and we rewrite (31) as

$$\psi^{(2)}_{-\omega_1, -\omega_2}(t) = \frac{E_1^* E_2^*}{4\hbar^2} \sum_s \frac{(\mu_1)_{mn} (\mu_2)_{sm} [e^{-i\omega t} e^{i(\omega_{sn} - \omega_1 - \omega_2)t} - 1]}{(\omega_{mn} - \omega_1)(\omega_{sn} - \omega_1 - \omega_2)} |s\rangle \quad (32)$$

The probability of finding the atom in some state k at time t is $|\langle k | \psi(t) \rangle|^2$ so that the transition probability due to two-photon absorption is

$$P_k = |\langle k | \psi^{(2)}(t) \rangle|^2 \quad (33)$$

$$= \frac{|E_1|^2 |E_2|^2 (\mu_1)_{mn}^2 (\mu_2)_{km}^2 \sin^2[\frac{1}{2}(\omega_{kn} - \omega_1 - \omega_2)t]}{16\hbar^4 (\omega_{mn} - \omega_1)^2 [\frac{1}{2}(\omega_{kn} - \omega_1 - \omega_2)]} \quad (34)$$

We note that transitions occur to the state k which conserves energy, i.e., to that state where $E_k - E_n = \hbar(\omega_1 + \omega_2)$. If the normalized lineshape function for the transition $n \rightarrow k$ is $g(\omega_{kn})$ then the average value of P_k is obtained by multiplying (34) by $g(\omega_{kn})$ and integrating from $-\infty$ to ∞ . Using

$$\lim_{t \rightarrow \infty} \frac{\sin^2 \frac{xt}{2}}{(x/2)^2} \rightarrow 2\pi t \delta(x) \quad (35)$$

we obtain for the transition rate

$$W_{n \rightarrow k} = \frac{d}{dt} P_k = \frac{\pi |E_1|^2 |E_2|^2 (\mu_1)_{mn}^2 (\mu_2)_{mk}^2 g(\omega_{kn} = \omega_1 + \omega_2)}{8\hbar^4 (\omega_{mn} - \omega_1)^2} \quad (36)$$

The special case of one frequency two-photon absorption where $\omega_1 = \omega_2$ has been considered in some detail⁽⁵⁾. We may obtain the absorption coefficient for this case by equating the change in the intensity I_ω of E_1 to

the number of transitions per unit time per unit volume.

$$\frac{dI_\omega}{dz} = 2\hbar\omega W_{n \rightarrow k} (N_k - N_n) \quad (37)$$

where I_ω is the intensity (watts/m²) at ω and N_k and N_n are the population densities of level k and n , respectively. Using $I_\omega = \frac{\epsilon c}{n_1} |E_1|^2 / 2$ we obtain

$$\alpha_{\text{two photon}} = \frac{\pi\omega(N_n - N_k)(\mu_1)_{mn}^2(\mu_1)_{km}^2 n_1^2 g(\omega_{kn}=2\omega) I_\omega}{\hbar^3(\omega_{mn}-\omega)^2 \epsilon^2 c^2} \quad (38)$$

IV. Raman Processes

As the most detailed example of the diagram formalism we take the case of Raman processes in which an atom initially in the ground state n absorbs a photon at ω_1 , emits one at ω_2 , while making a transition to the state k . The situation is depicted in Fig. 4. The situation is identical to that considered in the previous section, except that here the second photon at ω_2 is emitted rather than absorbed. This causes the ω_2 arrow in the Feynman diagram of Fig. 4 to have the opposite sense to that in Fig. 3. We can use directly the result of Section III and merely reverse the sign of ω_2 . Using (34) we obtain for the transition probability

$$P_k(t) = \frac{|E_1|^2 |E_2|^2 (\mu_1)_{mn}^2 (\mu_2)_{km}^2}{16\hbar^4 (\omega_{mn} - \omega_1)^2} 2\pi t \delta(\omega_{kn} - \omega_1 + \omega_2) \quad (39)$$

In (39) it was assumed that one term m dominates, so that the summation over m is omitted. As in (38) we introduce the normalized Raman line-shape function $g(\omega_{kn})$ such that $g(\omega_{kn})d\omega_{kn}$ is the probability of having ω_{kn} within the interval $d\omega_{kn}$. Multiplying (39) by $g(\omega_{kn})d\omega_{kn}$ and integrating leads to

$$P_k(t) = \frac{\pi t}{8\hbar^4} \frac{|E_1|^2 |E_2|^2 (\mu_1)_{mn}^2 (\mu_2)_{km}^2}{(\omega_{mn} - \omega_1)^2} g(\omega_{kn} = \omega_1 - \omega_2) \quad (40)$$

and a corresponding transition rate

$$W_{n \rightarrow k} = \frac{dP_k}{dt} = \frac{\pi}{8\hbar^4} \frac{|E_1|^2 |E_2|^2 (\mu_1)_{mn}^2 (\mu_2)_{km}^2}{(\omega_{mn} - \omega_1)^2} g(\omega_{kn} = \omega_1 - \omega_2) \quad (41)$$

$$= \frac{\pi n_1 n_2 I_1 I_2 (\mu_1)_{mn}^2 (\mu_2)_{km}^2}{2\hbar^4 c^2 \epsilon_1 \epsilon_2 (\omega_{mn} - \omega_1)^2} g(\omega_{kn} = \omega_1 - \omega_2) \quad (42)$$

where I is the intensity and ϵ_1 and ϵ_2 the dielectric constants at ω_1 and ω_2 , respectively and n_1 and n_2 are the refractive indices.

The exponential gain coefficient describing the amplification of the field at ω_2 is obtained from

$$\frac{dI_2}{dz} = g_{R1} I_2 = W_{n \rightarrow k} (N_n - N_k) \hbar \omega_2$$

which, using (42) gives

$$g_{R1} = \frac{\pi n_1 n_2 \omega_2 (\mu_1)_{mn}^2 (\mu_2)_{km}^2 (N_n - N_k) I_1}{2\hbar^3 c^2 \epsilon_1 \epsilon_2 (\omega_{mn} - \omega_1)^2} g(\omega_{kn} = \omega_1 + \omega_2) \quad (43)$$

Next we will describe the same Raman scattering leading to (43) by a different approach. Instead of using the concept of a transition rate we will calculate the induced dipole moment at ω_2 of an atom interacting with the ω_1 and ω_2 fields. To make sure that we will treat the problem to the same order of interaction we look for a dipole moment cubic in the applied field amplitudes.

$$\langle \mu_i \rangle \propto E_1 E_1^* E_2 e^{i(\omega_1 - \omega_1 + \omega_2)t} = |E_1|^2 E_2 e^{i\omega_2 t}$$

Such a contribution to μ_i which involves the third power of E can come from combinations such as $\langle \psi^{(1)} | \mu_i | \psi^{(2)} \rangle$, $\langle \psi^{(0)} | \mu_i | \psi^{(3)} \rangle$. An examination of (22) and (25) shows that the largest dipole moment will arise from the use of

$$\langle \mu_i \rangle = \langle \psi^{(1)}(t) | \mu_i | \psi^{(2)} \rangle + \text{c.c.} \quad (44)$$

where taking the direction of \vec{E}_1 as j and \vec{E}_2 as z

$$\psi^{(1)}(t) = \sum_m \left(\frac{i}{2\hbar} \right) \frac{E_1^* (\mu_1)_{mn}}{(\omega_{mn} - i\gamma_m - \omega_1)} e^{i(-\omega_1 - \omega_n)t} |m\rangle \quad (45)$$

$$\psi^{(2)}(t) = \sum_g \sum_s \frac{E_1^* E_2 (\mu_1)_{gn} (\mu_2)_{sg}}{4\hbar^2 (\omega_{gn} - \omega_1 - i\gamma)(\omega_{sn} - \omega_1 + \omega_2 - i\gamma)} e^{i(-\omega_1 + \omega_2 - \omega_n)t} |s\rangle \quad (46)$$

so that using (44),

$$\langle \mu_i \rangle = \frac{1}{8\hbar^3} \sum_m \sum_g \sum_s E_1 E_1^* E_2 \frac{(\mu_1)_{mn} (\mu_i)_{ms} (\mu_1)_{gn} (\mu_2)_{sg}}{(\omega_{mn} - \omega_1)(\omega_{gn} - \omega_1)(\omega_{sn} - \omega_1 + \omega_2 - i\gamma)} e^{i\omega_2 t} + \text{c.c.} \quad (47)$$

where we dropped the term $i\gamma$ in the first two factors in the denominators.

These must be reintroduced if operation is such that $\omega_{mn} \approx \omega_1$ or $\omega_{gn} \approx \omega_1$.

We will assume that the summation over m is dominated by one term where $\omega_{mn} \approx \omega_1$. Also, that ω_1 and ω_2 are chosen so that for some level $s = k$ $\omega_{kn} = \omega_1 - \omega_2$. We thus simplify (47) to

$$\langle \mu_i \rangle = \frac{1}{8\hbar^3} \frac{(\mu_1)_{mn}^2 (\mu_i)_{mk} (\mu_2)_{kn}}{(\omega_{mn} - \omega_1)^2 (\omega_{kn} - \omega_1 + \omega_2 + i\gamma)} e^{i\omega_2 t} E_1 E_1^* E_2 + \text{c.c.} \quad (48)$$

We define a nonlinear Raman susceptibility by

$$P_i^{(\omega_2)} = N \langle \mu_i \rangle = \epsilon_0 X_R |E_1|^2 E_2 \quad (49)$$

where $P^{(\omega_2)}$ is the complex amplitude of the polarization at ω_2 . From (48) and (49) we obtain

$$X_R = \frac{N}{4\hbar^3 \epsilon_0} \frac{(\mu_1)_{mn}^2 (\mu_i)_{mk} (\mu_2)_{mk}}{(\omega_{mn} - \omega_1)^2 (\omega_{kn} - \omega_1 + \omega_2 - i\gamma)} \quad (50)$$

The average power per unit volume generated at ω_2 is

$$p = - \frac{\omega \epsilon_0}{2} |E_2|^2 |E_1|^2 X_R'' \quad (51)$$

$$\text{where } X_R = X_R' - iX_R'' \quad (52)$$

An examination of (50) shows that when $\gamma = 0$ X_R is real and $p = 0$. The convergence factor γ in the Feynman formalism is thus fundamentally related to the problem of power dissipation. Let us for a moment consider γ as a parameter and calculate the power p . We obtain

$$X_R' = \frac{N}{4\hbar^3 \epsilon_0} \frac{(\mu_1)_{mn}^2 (\mu_i)_{mk} (\mu_2)_{mk} [\omega_{kn} - (\omega_1 - \omega_2)]}{(\omega_{mn} - \omega_1)^2 [(\omega_{kn} - \omega_1 + \omega_2)^2 + \gamma^2]} \quad (53)$$

$$X_R'' = \frac{-N}{4\hbar^3 \epsilon_0} \frac{(\mu_1)_{mn}^2 (\mu_i)_{mk} (\mu_2)_{mk} \gamma}{(\omega_{mn} - \omega_1)^2 [(\omega_{kn} - \omega_1 + \omega_2)^2 + \gamma^2]}$$

and from (51) (putting $i=2$ since only the polarization component along \vec{E}_2 contributes to absorption)

$$p = \frac{\omega_2}{8\hbar^3} |E_1|^2 |E_2|^2 \frac{(\mu_1)_{mn}^2 (\mu_2)_{mk}^2 \gamma}{(\omega_{mn} - \omega_1)^2 [(\omega_{kn} - \omega_1 + \omega_2)^2 + \gamma^2]} \quad (54)$$

This power must be the same as that calculated using the transition rate approach leading to (41). The latter leads to

$$\begin{aligned}
 p &= NW_{n \rightarrow k} \hbar \omega_2 \\
 &= \frac{N\pi\omega_2}{8\hbar^3} \frac{|E_1|^2 |E_2|^2 (\mu_1)_{mn}^2 (\mu_2)_{km}^2}{(\omega_{mn} - \omega_1)^2} g(\omega_{kn} = \omega_1 - \omega_2)
 \end{aligned} \tag{55}$$

Equating (54) to (55) and taking $\mu_1 = \mu_2$ gives

$$\frac{\gamma/\pi}{[\omega_{kn} - (\omega_1 - \omega_2)]^2 + \gamma^2} = g[\omega_{kn} - (\omega_1 - \omega_2)] \tag{56}$$

We thus obtained an explicit expression for the transition lineshape function $g[\omega_{kn} - (\omega_1 - \omega_2)]$. We now find that the result of the coherent treatment in which the problem is treated by the induced dipole agrees exactly with the transition rate approach if we merely regard γ as the Lorentzian width of the $k \rightarrow n$ transition.

V. Two-Photon Raman Processes

As the last application of the evolution operator techniques we consider the problem of two-photon Raman transitions of the type considered in Fig. 5. These processes were described by Yatsiv et al.⁽⁶⁾. We shall expand this discussion and show how these processes can be described in the formalism of nonlinear optics.

In the first of these processes (5a) one photon at ω_1 and one photon at ω_2 are absorbed and a photon at ω_3 is emitted, while the atom (molecule) makes a transition from the initial state n to some final state k . In the second process one photon (ω_1) is absorbed while photons ω_2 and ω_3 are emitted during the same transition.

The analysis of both these processes is similar and the results for 5b can be obtained from those of 5a by reversing the sign of ω_2 .

Using the formalism of nonlinear optics, the scattering events of Fig. 5 can be represented by

$$p_{\omega_3=\omega_1-\omega_1+\omega_2-\omega_2+\omega_3} = \epsilon_0 \chi_{R2}^{(\omega_3=\omega_1-\omega_1+\omega_2-\omega_2+\omega_3)} |E_1|^2 |E_2|^2 E_3 \quad (57)$$

so that we may expect an amplification (or attenuation) at ω_3 with an exponential constant proportional to $|E_1|^2 |E_2|^2$ in analogy with the one-photon Raman process (43). Alternatively, we can, as in Section IV, obtain the gain by calculating the transition rate per atom for the process illustrated in Fig. 5a.

By direct analogy with the calculation leading to (39) we obtain for the probability $P_k(t)$ of finding an atom in state k

$$P_k = |\langle k | \psi^{(3)}(t) \rangle|^2 = \frac{|E_1|^2 |E_2|^2 |E_3|^2 (\mu_1)_{mn}^2 (\mu_2)_{ms}^2 (\mu_3)_{sk}^2}{2^6 \hbar^6 (\omega_{mn} - \omega_1)^2 (\omega_{sn} - \omega_1 - \omega_2)^2} 2\pi t \delta(\omega_{kn} - \omega_1 - \omega_2 + \omega_3) \quad (58)$$

so that the transition rate $W_{n \rightarrow k}$ is

$$W_{n \rightarrow k} = \frac{\pi I_1 I_2 I_3 (\mu_1)_{mn}^2 (\mu_2)_{ms}^2 (\mu_3)_{sk}^2 n_1 n_2 n_3 I_1 I_2}{4 \hbar^6 c^3 \epsilon^3 (\omega_{mn} - \omega_1)^2 (\omega_{sn} - \omega_1 - \omega_2)^2} g(\omega_{kn} = \omega_1 + \omega_2 - \omega_3) \quad (59)$$

The power per unit volume generated at ω_3 is thus

$$p(\omega_3) = W_{n \rightarrow k} N_n \hbar \omega_3 = g_{R2} I_3 \quad (60)$$

where the two-photon Raman gain g_{R2} is

$$g_{R2} = \frac{N_n \pi \omega_3 (\mu_1)_{mn}^2 (\mu_2)_{ms}^2 (\mu_3)_{sk}^2 I_1 I_2}{4 \hbar^5 c^3 \epsilon^3 (\omega_{mn} - \omega_1)^2 (\omega_{sn} - \omega_1 - \omega_2)^2} g(\omega_{kn} = \omega_1 + \omega_2 - \omega_3) \quad (61)$$

and is thus proportional to the product of intensities at ω_1 and ω_2 .

We note by comparison to the expression (43) for the one-photon (i.e., conventional) Raman gain g_{R1} that

$$g_{R2} \approx g_{R1} \frac{\mu^2 I_2 n_3}{2\hbar^2 c \epsilon (\omega_{sn} - \omega_1 - \omega_2)^2} \quad (62)$$

If we assume that $I_2 \sim 10^6$ watt/cm, $(\omega_{sn} - \omega_1 - \omega_2) \sim 10^{10}$, i.e., near resonant tuning, $\mu \sim 10^{-30}$ MKS, we obtain

$$g_{R2} \approx g_{R1}$$

so that, using intense laser sources tuned near atomic resonances, it may be possible to obtain two-photon Raman gain approaching those of normal Raman processes.

Unlike frequency addition and multiplication, this process does not require phase matching. This is due to the fact that if the spatial phase factors are included in (57) they will cancel out, since each field amplitude is multiplied by its complex conjugate except for E_3 . The induced polarization $P^{(\omega_3)}$ thus has the same spatial phase as E_3 and the interaction is spatially cumulative. If the interaction region is provided with feedback, oscillation at ω_3 may result.

To describe the same process using the concept of nonlinear Raman susceptibility, we proceed to derive the dipole moment per atom $\langle \mu_i \rangle$ at ω_3 induced in the presence of fields at ω_1 , ω_2 , and ω_3 . Resonant contributions to the fifth order dipole moment arise from

$$\langle \mu_i \rangle = \langle \psi_{-\omega_1, -\omega_2}^{(2)} | \mu_i | \psi_{-\omega_1, -\omega_2, \omega_3}^{(3)} \rangle + \text{c.c.} \quad (63)$$

From (25) and (26) we obtain

$$\psi_{-\omega_1, -\omega_2}^{(2)}(t) = \sum_g \sum_s \left(\frac{1}{2\hbar} \right)^2 \frac{E_1^* E_2^* e^{i(-\omega_1 - \omega_2 - \omega_n)t}}{(\omega_{gn} - \omega_1 - i\gamma)(\omega_{sn} - \omega_1 - \omega_2 - i\gamma)} (\mu_1)_{ng} (\mu_2)_{gs} |s\rangle$$

$$\psi_{-\omega_1, -\omega_2, \omega_3}^{(3)}(t) = \frac{1}{8\hbar^3} \sum_{\ell} \sum_m \sum_k \frac{E_1^* E_2^* E_3 e^{i(-\omega_1 - \omega_2 + \omega_3 - \omega_n)t} (\mu_1)_{n\ell} (\mu_2)_{\ell m} (\mu_3)_{mk}}{(\omega_{\ell n} - \omega_1 - i\gamma)(\omega_{mn} - \omega_1 - \omega_2 - i\gamma)(\omega_{kn} - \omega_1 - \omega_2 + \omega_3 - i\gamma)} |k\rangle \quad (64)$$

so that

$$\langle \mu_i \rangle = \left(\frac{1}{32\hbar^5} \right) \sum_{gs \ell m k} \frac{|E_1|^2 |E_2|^2 E_3 (\mu_1)_{n\ell} (\mu_2)_{\ell m} (\mu_3)_{mk} (\mu_i)_{sp} e^{i\omega_3 t}}{(\omega_{\ell n} - \omega_1 - i\gamma)(\omega_{mn} - \omega_1 - \omega_2 - i\gamma)(\omega_{kn} - \omega_1 - \omega_2 + \omega_3 - i\gamma)(\omega_{gn} - \omega_1 + i\gamma)(\omega_{sn} - \omega_1 - \omega_2 + i\gamma)} + c.c. \quad (65)$$

Let us assume that ω_1 and ω_2 are adjusted so that for some levels ℓ and m , $\omega_{\ell n} \approx \omega_1$ while $\omega_{mn} \approx \omega_1 + \omega_2$. Also, that a level k exists such that $\omega_{kn} \approx \omega_1 + \omega_2 - \omega_3$. Keeping only the resonant term of (65) we obtain

$$\langle \mu_i \rangle \approx \frac{1}{32\hbar^5} \frac{|E_1|^2 |E_2|^2 E_3 (\mu_1)_{\ell n}^2 (\mu_2)_{\ell m}^2 (\mu_3)_{mk} [\omega_{kn} - (\omega_1 + \omega_2 - \omega_3 - i\gamma_{kn})] e^{i\omega_3 t}}{[(\omega_{\ell n} - \omega_1)^2 + \gamma_{\ell n}^2][(\omega_{mn} - \omega_1 - \omega_2)^2 + \gamma_{mn}^2][\{\omega_{kn} - (\omega_1 + \omega_2 - \omega_3)\}^2 + \gamma_{kn}^2]} + c.c. \quad (66)$$

If we relate the complex amplitude $P_i(\omega_3)$ of the induced polarization $N\langle \mu_i \rangle$ to the complex field amplitudes via

$$P_i^{(\omega_3)} = \epsilon_0 \chi_{R2} |E_1|^2 |E_2|^2 E_3, \quad \chi_{R2} = \chi'_{R2} - i\chi''_{R2} \quad (67)$$

we obtain

$$\chi'_{R2} = \frac{N}{16\hbar^5 \epsilon_0} \frac{(\mu_1)_{\ell n}^2 (\mu_2)_{\ell m}^2 (\mu_3)_{mk} (\mu_i)_{mk}}{[(\omega_{\ell n} - \omega_1)^2 + \gamma_{\ell n}^2][(\omega_{mn} - \omega_1 - \omega_2)^2 + \gamma_{mn}^2]} \frac{[\omega_{kn} - (\omega_1 + \omega_2 - \omega_3)]}{[\{\omega_{kn} - (\omega_1 + \omega_2 - \omega_3)\}^2 + \gamma_{pn}^2]}$$

$$\chi''_{R2} = - \frac{N}{16\hbar^5 \epsilon_0} \frac{(\mu_1)_{\ell n}^2 (\mu_2)_{\ell m}^2 (\mu_3)_{mk} (\mu_i)_{mk} \gamma_{pn}}{[(\omega_{\ell n} - \omega_1)^2 + \gamma_{\ell n}^2][(\omega_{mn} - \omega_1 - \omega_2)^2 + \gamma_{mn}^2][\{\omega_{kn} - (\omega_1 + \omega_2 - \omega_3)\}^2 + \gamma_{pn}^2]} \quad (68)$$

where $2\gamma_{ij}$ is the full width at half maximum of the $i \rightarrow j$ transition.

It follows immediately that the presence of a negative χ_{R2}'' causes an amplification at ω_3 with an exponential gain constant⁽⁷⁾

$$g_{R2} = -\frac{\omega_3}{cn_3} \chi_{R2}'' |E_1|^2 |E_2|^2 \quad (69)$$

$$= \frac{N\pi\omega_3(\mu_1)_{\ell n}^2(\mu_2)_{\ell m}^2(\mu_3)_{mk}^2 n_1 n_2 n_3 I_1 I_2}{4\hbar^5 c^3 \epsilon_1 \epsilon_2 \epsilon_3 [(\omega_{\ell n} - \omega_1)^2 + \gamma_{\ell n}^2][(\omega_{mn} - \omega_1 - \omega_2)^2 + \gamma_{mn}^2]} \frac{\gamma_{kn}/\pi}{[\{\omega_{kn} - (\omega_1 + \omega_2 - \omega_3)\}^2 + \gamma_{kn}^2]} \quad (70)$$

where we used $I_i = c\epsilon_i |E_i|^2 / 2n_i$. The result (70) for g_{R2} is identical with (61) once we associate the second factor in (70) with the normalized lineshape function $g[\omega_{kn} - (\omega_1 + \omega_2 - \omega_3)]$.

We thus find that the gain exercised by the wave E_3 is proportional to the product $I_1 I_2$ of the intensities at ω_1 and ω_2 , so that a stimulated Raman emission at ω_3 may be expected at some critical value of $I_1 I_2$.

The analysis of the two photon (emissive) Raman process shown in Fig. 5b is similar. All we need to do to obtain the gain at ω_3 is to replace ω_2 by $-\omega_2$. A fundamental difference between the two processes, however, would be revealed had we considered the consequence of the quantized nature of the field operators. The temporal rate of the photon number at ω_3 corresponding to process 5a is

$$\frac{dn_3}{dt} = C_1 n_1 n_2 (n_3 + 1) \quad (71)$$

while that of 5b is

$$\frac{dn_3}{dz} = \frac{dn_2}{dz} = C_2 n_1 (n_2 + 1) (n_3 + 1)$$

where n_i is the number of photons at ω_i , C_1 and C_2 are rate constants.

It follows immediately that the stimulated emission of photons in 5a

requires the simultaneous presence of the fields at ω_1 and ω_2 while in 5b stimulation can take place with a single input at ω_1 , since $dn_3/dz > 0$ when $n_3 = n_2 = 0$.

We may also note that the emissive two-photon Raman process of 5b can be used to generate long wavelength radiation at ω_3 .

To summarize, the formalism of time evolution operators and the related technique of Feynman diagrams was applied to a variety of multi-photon processes in nonlinear optics. The formalism affords relatively direct and orderly treatment of complicated high order processes.

References

1. A. Messiah, Quantum Mechanics II (Interscience Publ., New York, 1962), p. 724.
2. J. A. Armstrong, N. Bloembergen, J. Ducuing, and P. S. Pershan, "Interaction between Light Waves in a Nonlinear Dielectric", Phys. Rev. 127, 1918 (1962).
3. R. B. Miles and S. E. Harris, "Optical Third Harmonic Generation in Alkali Metal Vapors", IEEE J. Quant. Elect. QE-9, 470 (1973).
4. R. L. Abrams, A. Yariv, and P-C. Yeh, "Stark Induced Three-Wave Mixing in Molecular Liquids --Part I: Theory," IEEE J. Quant. Elect. QE-13, 79 (1977).
5. W. Kaiser and C.G.B. Garrett, Phys. Rev. 7, 229 (1961).
6. S. Yatsiv, M. Rokni and S. Barak, IEEE J. Quant. Elect. QE-4, 900 (1968).
7. A. Yariv, Quantum Electronics, 2nd Ed. (J. Wiley & Sons, Inc., New York, 1975), p. 487.

Figure Captions

- Fig. 1. The levels and frequencies involving a Raman scattering from state n to k .
- Fig. 2. The Feynman diagrams used to obtain: (a) $\psi_{-\omega_1, -\omega_2}^{(2)}(t)$, (b) $\psi_{-\omega_1, +\omega_2}^{(2)}(t)$, (c) $\psi_{-\omega_1, -\omega_2, \omega_3}^{(3)}(t)$.
- Fig. 3. Feynman diagram used in treating two-photon absorption.
- Fig. 4. Energy levels and Feynman diagrams involved in Raman scattering.
- Fig. 5. Energy levels and Feynman diagrams involved in two-photon Raman scattering

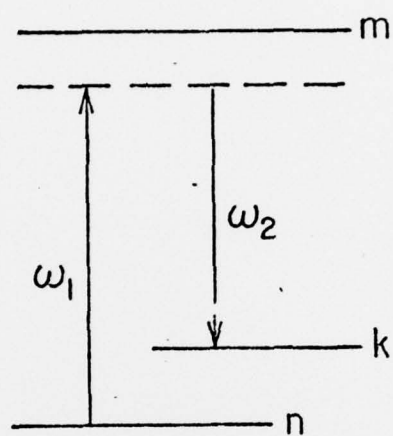


Fig 1
10/11

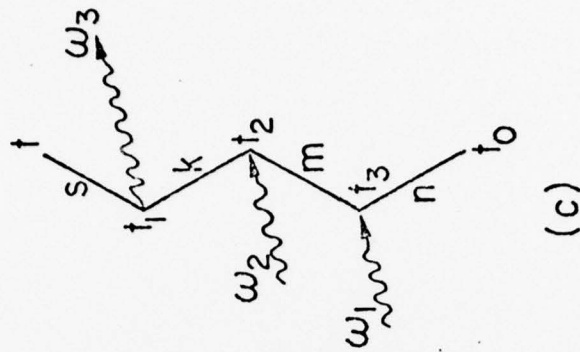
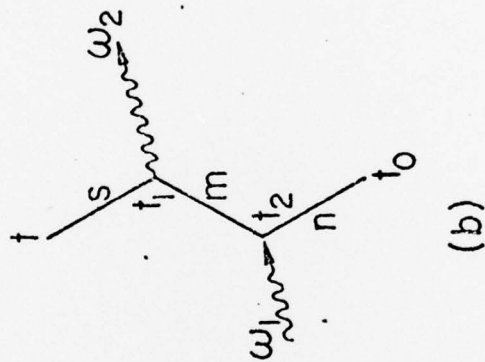
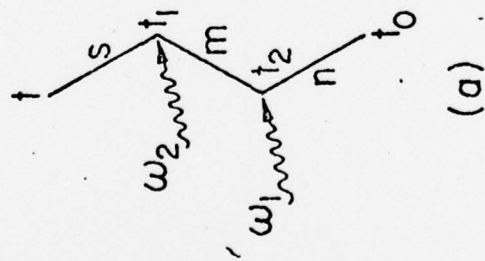


Fig. 2

197

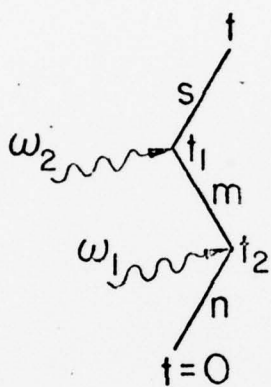


Fig 3

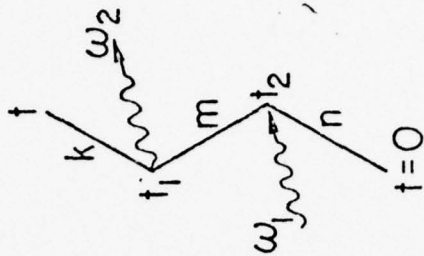
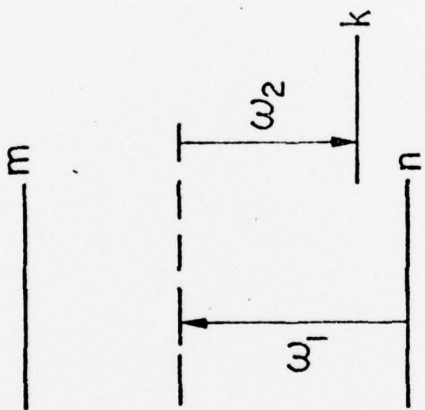
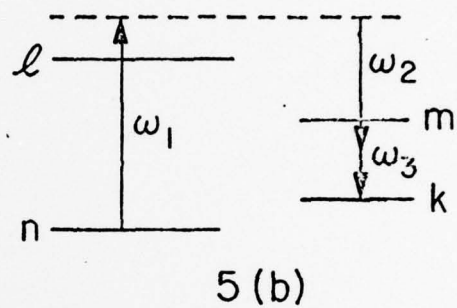
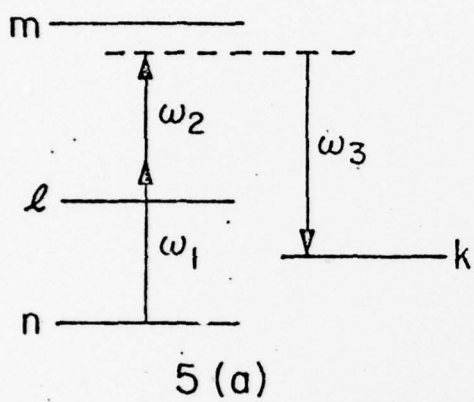


Fig 4



UNCLASSIFIED

SECURITY CLASSIFICATION OF THIS PAGE (When Data Entered)

REPORT DOCUMENTATION PAGE		READ INSTRUCTIONS BEFORE COMPLETING FORM
1. REPORT NUMBER FINAL TECHNICAL REPORT	2. GOVT ACCESSION NO.	3. RECIPIENT'S CATALOG NUMBER
4. TITLE (and Subtitle) ELECTROOPTIC PHENOMENA AND DEVICES IN GASES Final Report		5. TYPE OF REPORT & PERIOD COVERED Final Report 30 June 1975 - 29 June 1977
		6. PERFORMING ORG. REPORT NUMBER
7. AUTHOR(s) Amnon Yariv, Principal Investigator		8. CONTRACT OR GRANT NUMBER(s) DAAG29-75-G-0191 <i>new</i>
9. PERFORMING ORGANIZATION NAME AND ADDRESS California Institute of Technology Pasadena, California 91125		10. PROGRAM ELEMENT, PROJECT, TASK AREA & WORK UNIT NUMBERS
11. CONTROLLING OFFICE NAME AND ADDRESS		12. REPORT DATE Sept. 26, 1977
		13. NUMBER OF PAGES 35
14. MONITORING AGENCY NAME & ADDRESS (if different from Controlling Office)		15. SECURITY CLASS. (of this report)
		15a. DECLASSIFICATION/DOWNGRADING SCHEDULE
16. DISTRIBUTION STATEMENT (of this Report) Approved for public release; distribution unlimited.		
17. DISTRIBUTION STATEMENT (of the abstract entered in Block 20, if different from Report)		
18. SUPPLEMENTARY NOTES		
19. KEY WORDS (Continue on reverse side if necessary and identify by block number) mixing in NH_2D Time reversed propagation Nonlinear optics Phase conjugation		
20. ABSTRACT (Continue on reverse side if necessary and identify by block number) Theoretical analysis was performed on a number of problems in nonlinear optics including 3-photon mixing in gases in the presence of a dc electric field and 4-photon mixing leading to a time reversed phase conjugate wave propagation.		

DD FORM 1 JAN 73 1473

EDITION OF 1 NOV 65 IS OBSOLETE

UNCLASSIFIED

SECURITY CLASSIFICATION OF THIS PAGE (When Data Entered)